APPLIED ORGANOMETALLIC CHEMISTRY, VOL. 12, 419–426 (1998)

Optimized Structures of $Cr_2(CO)_6^+$ with Three Different Symmetries by Density Functional Calculation.

Takao Wada,[1] Satoru Nishio,[1]* Takayuki Yada,[1] Satoshi Hayashi,[1] Akiyoshi Matsuzaki,[1] Hiroyasu Sato,[1] Hisayoshi Kobayashi[2] and Tokio Yamabe[3]
[1]Department of Chemistry for Materials, Faculty of Engineering, Mi'e University, Kamihama-cho, Tsu, Mi'e 514, Japan
[2]Kurashiki University of Science and the Arts, 2640 Nishinoura, Tsurajima-cho, Kurashiki 712, Japan.
[3]Department of Molecular Engineering, Graduate School of Engineering, Kyoto University, Sakyoku, Kyoto 606-01, Japan

Density functional calculations have been made on a binuclear metal carbonyl ion $Cr_2(CO)_6^+$ found in our laser ablation–molecular beam (LAMB) experiment. Optimized structures are calculated for three different conformations: *T33* of D_{3d} symmetry with three terminal carbonyl groups on each chromium atom, *B2T22* of D_{2h} symmetry with two bridging carbonyl groups and two terminal carbonyl groups on each chromium atom, and *B4T11* of D_{4h} symmetry with four bridging carbonyl groups and one terminal carbonyl group on each chromium atom. The most stable conformation is *T33* which is 36.76 and 286.44 kJ mol^{-1} lower in energy than *B2T22* and *B4T11*, respectively. The difference of conformation exerts a significant influence on the internuclear distance between chromium and the carbon of terminal CO, but hardly on the Cr–Cr bond length. For *B2T22* and *B4T11*, longer C–O distances for bridging carbonyls compared with those for terminal ones indicate effective π^*-back donation from the chromium atom to the bridging carbonyl groups. Furthermore, the relative abundance of $Cr_2(CO)_n^+$ (n = 0–6) observed in our previous experimental study can be explained qualitatively by comparison of the excess energy produced in the formation of a Cr^+–Cr bond with the CO dissociation energy of $Cr_2(CO)_6^+$. © **1998 John Wiley & Sons, Ltd.**

Appl. Organometal. Chem. **12**, 419–426 (1998)

* Correspondence to: Satoru Nishio, Department of Chemistry for Materials, Faculty of Engineering, Mi'e University, Kamihama-cho, Tsu, Mi'e 514, Japan.
E-mail: nishio@chem.mie-u.ac.jp
Contract/grant sponsor: Ministry of Education, Science and Culture, Japan; Contract/grant number: Specially Promoted Research 07102009.

Keywords: density functional calculation; binuclear metal carbonyl; $Cr_2(CO)_6^+$; laser ablation; molecular beam; optimized structures; dissociation energy

Received 4 July 1997; accepted 5 January 1998

1 INTRODUCTION

Metal carbonyl complexes have been widely studied both from the experimental and theoretical points of view, since they are promising heterogeneous catalysts or useful reactants for chemical vapor deposition (CVD) from the practical aspect, and are also important as model systems in surface and material science on the fundamental side.[1] Along with this trend, a new technology named the laser ablation–molecular beam (LAMB) method has been developed in our laboratory to prepare a variety of novel binuclear carbonyl complex ions $MCr(CO)_n^+$ (M = Ti, V, Cr, Mn, Fe; n = 0–6) which are coordinatively unsaturated. In this method, various metal ions (M^+) laser-ablated from the metal surface are allowed to react with $Cr(CO)_6$ in a molecular beam injected nearby.[2] Mass-spectroscopic studies with a quadrupole mass-selection apparatus have shown strong M dependence on the numbers of coordinated carbonyl groups.

Molecular structures of these novel metal carbonyls are very interesting. Low yields, however, prohibit their experimental determination. Therefore, we have performed computer calculations to obtain information on the structures of these compounds.

Recent progress in the processing capabilities of

 CCC 0268–2605/98/060419–08 $17.50

computers together with the well-organized availability of quantum chemistry programs, such as *ab initio*, Xα and density functional (DF) methods, makes possible calculations of these binuclear complexes. It is common knowledge, in particular, that the DF method is superior to *ab initio* calculations in computational expedience as well as in conformity with various experimental results.[3–7] Making the best use of these advantages the DF method has been successful for large molecules containing transition metals. Structures and energies have been studied by the DF method, so far, for various metal carbonyl complexes, including large binuclear ones.[4]

In view of the current position, we have performed DF calculations to determine structures and energies of the binuclear metal carbonyl complex ions $MCr(CO)_n^+$ (M = Ti, V, Cr, Mn, Fe; n = 0–6) obtained in our LAMB experiments. In this report, DF calculations are carried out on $Cr_2(CO)_6^+$. Furthermore, the relative abundance of $Cr_2(CO)_n^+$ (n = 0–6) observed in our previous experiments is explained qualitatively by comparison of the excess energy produced in the formation of a Cr^+–Cr bond with the dissociation energy for CO from $Cr_2(CO)_6^+$.

2 CALCULATION

2.1 Method

The method used here is based on the Kohn–Sham equations and density functional theory.[8,9] The spin orbitals, charge density and exchange-correlation (XC) potential are expanded using sets of Cartesian Gaussian functions and the XC energy is evaluated by numerical integration on a grid.

A DF program based on 'deMon', developed by St-Amant and Salahub[10,11] and modified by Kobayashi[12,13] is applied. In all calculations reported here, the self-consistent equations are solved using the non-local XC potential with correction to exchange as proposed by Becke[14] and to correlation following Perdew.[15] Geometry optimizations are started at the initial geometry with the results of extended Hückel molecular orbital calculations. They are performed by a standard method (Broyden–Fletcher–Goldfarb–Shanno) for minimizing the norm of the LCGTO-DF gradient as reported by Fournier.[3] The stationary points are characterized by evaluating the energy second derivatives by finite difference of analytical gradients. The orbital basis sets applied are the characterized contraction pattern (63321/531*/41+) for chromium and the pattern (5211/411) for carbon and oxygen.[16] The auxiliary basis sets used here for fitting the density and XC potential consist of ten *s*, five *p* and five *d* uncontracted shells of functions for chromium and seven *s*, two *p* and two *d* for carbon and oxygen. DF calculations were performed on IBM RS/6000 and SGI 4D-Indy workstations.

In the present calculation, three different conformations of $Cr_2(CO)_6^+$ ions belonging to relatively high-symmetry groups D_{3d}, D_{2h} and D_{4h} as shown in Fig. 1 are adopted: (1) *T33* of D_{3d} symmetry with three terminal carbonyl groups on two chromium atoms with the two $Cr(CO)_3$ moieties mutually eclipsed; (2) *B2T22* of D_{2h} symmetry with two bridging carbonyl groups and two terminal carbonyl groups on each chromium atom; and (3) *B4T11* of D_{4h} symmetry with four bridging carbonyl groups and one terminal carbonyl group on each chromium atom. Spin multiplicity is fixed at doublet for each complex ion in this study in view of the finding that *T33* with spin multiplicity $S = 2$ (doublet) was more stable (−2768.5482 hartree) than that with $S = 4$ (quartet) (−2768.5452 hartree).

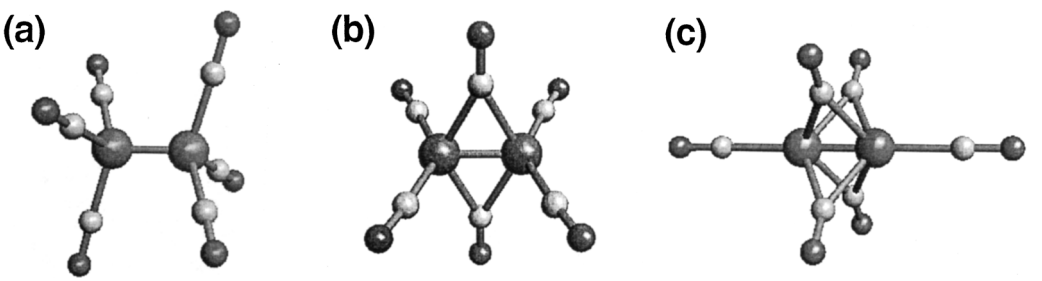

Figure 1 Three conformations in this study for $Cr_2(CO)_6^+$ ions, (a) *T33* with D_{3d} symmetry, (b) *B2T22* with D_{2h} symmetry, (c) *B4T11* with D_{4h} symmetry.

Table 1 Structural parameters for $Cr(CO)_6$ and Cr_2 and CO dissociation energy of $Cr(CO)_6$

					A-Mol[c]		ADF[d]		
	Our result	HFS[a]	DMol[b]	DGauss[b]	LDA[e]	LDA/NL[f]	TZ[g]	TZD[h]	Experimental
$Cr(CO)_6$									
R(Cr–C) (Å)	1.889	1.868	1.869	1.867	1.872	1.909	—	—	1.914[i]
R(C–O) (Å)	1.186	1.143	1.157	1.159	1.141	1.153	1.179	1.155	1.140[i]
D(Cr–C) (kJ mol^{-1})	183	278	—	—	276	147	175.2	170.7	162[i]
Cr_2									
R(Cr–Cr) (Å)	1.664	—	—	—	—	—	—	—	1.68[j]

[a] Reference 18. HFS, Hartree–Fock–Slater.
[b] Reference 19. DMol, DGauss.,
[c] Reference 20. A-Mol.,
[d] Reference 21.
[e] Local density approximation.
[f] Non-local density functional method.
[g] Using TZ basis set in ADF program.
[h] Using TZD basis set in ADF program.
[i] Reference 17.
[j] Reference 22.

2.2 Reliability of our calculation

In order to confirm the accuracy of our calculations, optimized structures and energies are calculated in advance for neutral $Cr(CO)_6$, and Cr_2, both of which are widely studied from theoretical and experimental aspects. Internuclear distances between Cr and C and between C and O for $Cr(CO)_6$ [R(Cr–C) and R(C–O), respectively], the dissociation energy of CO from $Cr(CO)_6$ [D(Cr–CO)] and the internuclear distance between Cr atoms for Cr_2 [R(Cr–Cr)] are listed in Table 1 together with those determined in several other theoretical and experimental studies. According to our calculation, R(Cr–C) is 1.889 Å. This value is well consistent with values determined by experiment (1.914 Å),[17] being by no means inferior to those calculated by several methods.[18–21] Against the quite excellent result for R(Cr–C), R(C–O) by our calculation is 1.186 Å, which is rather overestimated. This is probably due to the lack of a polarization function in the basis set applied for C and O in our calculation. Rosa *et al.* calculated R(Cr–C) and R(C–O) of $Cr(CO)_6$ using several basis sets.[21] They have reported that adding a *d* polarization function improved the calculated C–O bond length, although only minor differences could be seen for R(Cr–C) among the ligand basis sets. (Strictly speaking, a slight lengthening of the bond due to the *d* polarization function is observed.) Actually our preliminary calculation shows that the internuclear distance between C and O for free CO calculated using the (5211/411) set without a *d* polarization function is long (1.175 Å) compared with the experimental value (1.128 Å) although the value calculated using the (5211/411/1) set with the *d* polarization functions is considerably improved (1.148 Å). The large sizes of the subjects of our investigation (containing two transition-metal atoms and six carbonyl groups) prevents us from choosing larger basis sets with polarization functions. Although D(Cr–CO) obtained by our calculation (183 kJ mol^{-1}) is larger than the experimental value, it is comparable with a value obtained by other DF calculations in a self-consistent non-local density functional (LDA/NL) method and much better than those obtained by the Hartree–Fock–Slater (HFS) method and DF at local density approximation (LDA) level. R(Cr–Cr) by our calculation (1.664 Å) is in good agreement with that determined by experiment.[22]

3 RESULTS AND DISCUSSION

3.1 Optimized structures and total energies for *T33*, *B2T22* and *B4T11*

Internuclear distances and total energies of the optimized structure for each conformation are listed in Table 2, where *R(*A–B*)* is an internuclear distance between atoms A and B, and C_T and C_B are carbon atoms in terminal and bridging carbonyl groups, respectively. Atomic populations (APs) on each atom, and atomic bond populations (ABPs) between adjacent atoms, are listed in Tables 3 and 4, respectively.

Table 2 Calculated internuclear distances, bond angles and total energies of optimized structures calculated for *T33*, *B2T22* and *B4T11*

	T33	*B2T22*	*B4T11*
Distances (Å)			
R(Cr–Cr)	1.841	1.901	1.879
R(Cr–C_T)	1.930	1.973	2.169
R(Cr–C_B)	—	2.084	2.141
R(C_T–O)	1.173	1.171	1.166
R(C_B–O)	—	1.191	1.185
Angles (degree)			
Cr-Cr-C_T	106.9	—	—
Cr-C_T-O	178.7	175.6	180.0
C_T-Cr-C_T	111.9	142.4	—
Cr-C_B-Cr	—	54.3	52.1
Cr-C_B-O	—	152.8	154.0
C_B-Cr-C_T	—	—	111.6
E (hartree)	−2768.5423	−2768.5283	−2768.4332

Table 3 Atomic population (AP) on each atom for *T33*, *B2T22* and *B4T11*

	Cr	C_T	C_B	O_T	O_B
T33	23.946	5.878	—	7.973	—
B2T22	23.934	5.836	5.949	8.002	8.000
B4T11	23.711	5.962	5.965	7.960	7.968

Table 4 Atomic bond population (ABP) between adjacent atoms for *T33*, *B2T22* and *B4T11*

	Cr–Cr	Cr–C_T	Cr–C_B	C_T–O	C_B–O
T33	0.083	0.253	—	0.517	—
B2T22	0.084	0.263	0.158	0.508	0.476
B4T11	−0.379	0.094	0.139	0.514	0.430

In our calculation, *T33* with a total energy of −2768.5423 hartree is the most stable structure among the three. *B2T22* and *B4T11* are 36.76 and 286.44 kJ mol^{-1} higher in energy than *T33*; respectively. The considerably high total energy for *B4T11* suggests the presence of only small amounts of $Cr_2(CO)_6^+$ with this conformation.

The internuclear distances between the two chromium atoms *R*(Cr–Cr) for *T33*, *B2T22* and *B4T11* are 1.841, 1.901 and 1.879 Å, respectively. The difference between the shortest and the longest ones is only 0.06 Å, indicating no strong dependence of *R*(Cr–Cr) on the coordination pattern of the carbonyl groups.

On the other hand, significant correlation can be observed between *R*(Cr–C_T) and the coordination pattern of the carbonyl groups. An increase in the number of C_BO from 0 (*T33*) via 2 (*B2T22*) to 4 (*B4T11*) results in the extension of *R*(Cr–C_T) to 1.930 Å, 1.973 Å and 2.169 Å, in that order. The difference between *B2T22* and *B4T11*, in particular, amounts to 0.196 Å. As a result, while *R*(Cr–C_T) is 0.111 Å shorter than *R*(Cr–C_B) in the case of *B2T22*, it is 0.028 Å longer for *B4T11*. Two primary factors directing *R*(Cr–C_T) can be conceived. If the C_TO approaches Cr along the Cr–Cr axis, strong repulsion should arise between Cr and C_TO, resulting in extension of *R*(Cr–C_T). According to our detailed analysis, the atomic orbital population of the singly occupied molecular orbital (SOMO) for *B4T11* is significantly high on the d_z orbital, indicating that the electron is indeed localized on the Cr–Cr axis. The other factor is the number of C_BO. The correlation between the remarkable extension of *R*(Cr–C_T) and the decrease in ABP between chromium atom and C_T (from 0.263 for *B2T22* to 0.094 for *B4T11*) with an increasing number of C_BOs indicates the strong interaction between the two chromium atoms and the C_BO attached to them. This is supported by the AP on each chromium atom, which decreases with increasing number of C_BOs from 23.946 (*T33*), via 23.934 (*B2T22*) to 23.711 (*B4T11*), indicating that the electron donating ability of the chromium atom is enhanced by increasing the number of C_BOs. It should be noted that the metal–metal bond is no longer formed in *B4T11*, considering the ABP between the chromium atoms (−0.379). The absence of direct metal–metal bonds in a binuclear metal complex is also reported by Bauschlicher.[23] He calculated the optimized structure of $Fe_2(CO)_9$ with D_{3h} symmetry using an SCF wavefunction with a large basis set to show that the bridging carbonyl groups hold the two $Fe(CO)_3$ fragments together by σ-donation into the empty Fe–Fe $d\pi$ orbital and metal donation from the $d\pi^*$ orbital into the carbonyl $2\pi^*$ orbital.

3.2 Dependence of internuclear distances of carbonyl groups (both C_BO and C_TO) on the number of C_BOs

Analysis of internuclear distances of carbonyl groups (both C_BO and C_TO) as a function of the number of C_BOs is of immense interest. *R*(C_T–O) values for *T33*, *B2T22* and *B4T11* are 1.173, 1.171 and 1.166 Å, respectively, decreasing gradually increasing number of C_BOs. This means that σ-forward and π^*-back donation between chromium and C_TO occurs more effectively for the complexes with smaller numbers of C_BOs. Furthermore, as for

B2T22 and *B4T11*, longer internuclear distances *R(*C_B–O*)* (1.191 and 1.185 Å for *B2T22* and *B4T11*, respectively), compared with *R(*C_T–O*)* (1.171 and 1.166 Å for *B2T22* and *B4T11*, respectively), suggest the effective σ-forward and π*-back donation between chromium and C_BO.

For binuclear metal carbonyl complexes, a longer internuclear distance of bridged CO than that of terminal CO is also shown by Ziegler *et al.*[4] in their DF calculation of $(CO)_4Co–Co(CO)_4$ with C_{2v} symmetry, where *R(*C_B–O*)* (1.169 Å) is 0.02 Å longer than *R(*C_T–O*)* (1.149 Å) in good agreement with experimental results (1.167 Å for *R(*C_B–O*)* and 1.136 Å for *R(*C_T–O*)*). Although both *R(*C_B–O*)* and *R(*C_T–O*)* for $(CO)_4Co–Co(CO)_4$ studied by Ziegler *et al.* are shorter than those for *B2T22* and *B4T11*, we cannot make a direct comparison between them since the basis set in our calculation is smaller than theirs with respect to polarization functions, as mentioned in the previous section.

AP and ABP results listed in Tables 3 and 4, respectively, allow us to give a qualitative explanation for the relationship between *R(*$C_{B,T}$–O*)* and the number of C_BOs in terms of the σ-forward and/or *-back donation. In *B2T22* and *B4T11*, larger APs on carbon atoms in C_BO (5.949 for *B2T22* and 5.965 for *B4T11*) than those on carbon atoms in C_TO (5.836 for *B2T22* and 5.962 for *B4T11*) indicate effective π*-back donation. In both cases, *B2T22* and *B4T11*, this is supported by comparison of the ABP in C_BO with that in C_TO. ABPs in C_BO (0.430 and 0.476 for *B4T11* and *B2T22*, respectively) are smaller than those in C_TO (0.514 and 0.508, for *B4T11* and *B2T22*, respectively). This is due to increased electron ejection from the chromium atom into the antibonding orbital of C_BO rather than that into C_TO.

We can explain qualitatively the difference between *R(*C_T–O*)* and *R(*C_B–O*)* in each *B2T22* and *B4T11* conformation in this analysis. However, more detailed analysis is necessary in order to clarify the difference in *R(*C_T–O*)* and in *R(*C_B–O*)* between the different conformations (*B2T22* and *B4T11*). In general, σ-forward donation occurs mainly by mixing a 5σ occupied orbital of free CO with an unoccupied 3*d*/4*s* hybrid orbital of the metal atom, and π*-back donation by mixing a 2π* unoccupied orbital of free CO with an occupied 3*d*/4*s* hybrid orbital of the metal atom, as shown in Fig. 2. The plane in the Figure is defined by the Cr–Cr axis and two bridging COs for *B4T11*. Figures 2(a) and 2(b) show the SOMO-1 level (the highest doubly occupied molecular orbital) participating in *-back donation and the SOMO-2 level participating in σ-forward donation between chromium atoms and bridging COs, respectively.

Table 5 Charge flowing out of carbonyl groups into chromium atoms by σ-forward donation (n_σ) and into carbonyl groups from chromium atoms by π*-back donation (n_{π^*}) for C_TO and C_BO in each conformation

	C_TO		C_BO	
	n_σ	n_{π^*}	n_σ	n_{π^*}
T33	0.516	0.368	—	—
B2T22	0.502	0.309	0.506	0.455
B4T11	0.216	0.138	0.505	0.439

Separation of the ABP into two portions respectively related to σ-forward and π*-back donation gives us further insight into *R(*$C_{B,T}$–O*)*. Table 5 lists the charge flowing out of the carbonyl group into the chromium atom by σ-forward donation (n_σ) and that into the carbonyl group from the chromium atom by π*-back donation (n_{π^*}) for each conformation. Here, n_σ and n_{π^*} are obtained by separation of the AP on carbon and oxygen into two portions related to σ-forward donation and π*-back donation and subtracting them from 10 (σ electrons of free CO) and 4 (π electrons of free CO), respectively. As for C_TO, both n_σ (0.216, 0.502 and 0.516 for *B4T11*, *B2T22* and *T33*, respectively) and n_{π^*} (0.138, 0.309 and 0.368 for *B4T11*, *B2T22* and *T33*, respectively) increase with decreasing number of C_BOs indicating that C_BOs restrict σ-forward and π*-back donation between chromium and C_TO. Both n_{π^*} values for C_BO in *B2T22* and *B4T11* (0.455 and 0.439, respectively) are larger than n_{π^*} for C_TO in every conformation, although n_σ for C_BO (0.443) is smaller than those for C_TO in *T33* and *B2T22*. π*-Back donation contributes more effectively to extension of the CO bond than σ-forward donation, because the 2π* unoccupied orbital of free CO participating in π*-back donation is an antibonding orbital while the 5σ orbital participating in σ-forward donation is primarily non-bonding (although the 5σ orbital is, strictly speaking, an antibonding orbital as a result of calculation, as shown in Fig. 2, the contribution to extension of CO bond is so small as to be negligible). Therefore, the internuclear distance of carbonyl groups is mainly governed by n_{π^*}.

3.3 The first Cr–CO bond dissociation energies of *T33*, *B2T22* and *B4T11*

In our previous LAMB experimental studies on formation of $Cr_2(CO)_n^+$(n = 0–6),[2] a peculiar

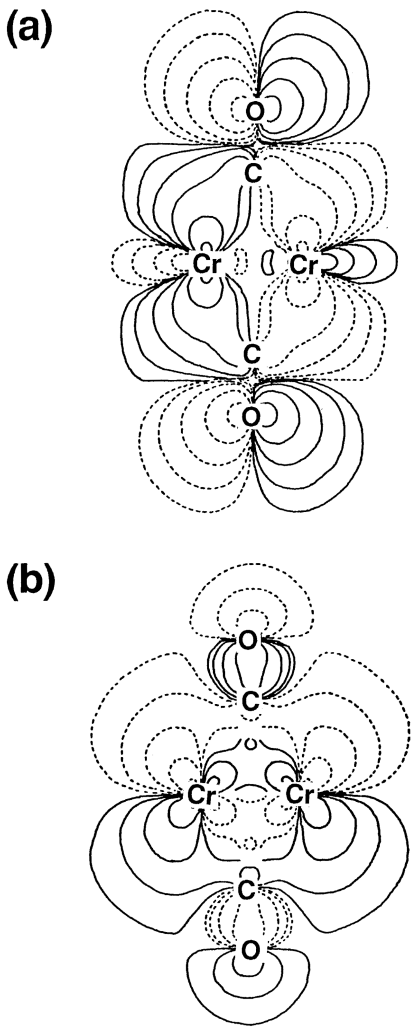

Figure 2 Contour plot of two orbital wave functions of (a) the SOMO-1 level (the highest doubly occupied molecular orbital) participating in π*-back donation and (b) the SOMO-2 level for *B4T11* participating in σ-forward donation between chromium atoms and carbonyl groups.

feature in the relative abundance of ions was observed where the amount of $Cr_2(CO)_5^+$ was larger than for any other $Cr_2(CO)_n^+$. In order to give an explanation for such an experimental finding, the first Cr–C_BO and –C_TO bond dissociation energies of *T33*, *B2T22* and *B4T11* in reaction [1] are estimated.

$$Cr_2(CO)_6^+ \rightarrow Cr_2(CO)_5^+ + CO \qquad [1]$$

The results are listed in Table 6. Each bond dissociation energy *D*(Cr–CO) is calculated by Eqn [2], where *E*[A] is the total energy of compound A. In this calculation, for simplicity, structural parameters except for the distance between the Cr and C of eliminated carbonyl groups are fixed at the values listed in Table 2 without geometry optimization for $Cr_2(CO)_5^+$ and dissociated CO. Therefore, the effect of relaxation of $Cr_2(CO)_5^+$ on stabilization is disregarded. Every CO bond dissociation energy is around 160 kJ mol^{-1} except for *B4T11*. In particular, the value for C_TO in *B4T11* is quite small (59.6 kJ mol^{-1}) compared to those for C_TOs in *T33* and *B2T22*. This small value is, as a matter of course, correlated closely with the ABP between Cr–C_T as shown in Table 4, indicating the weak bonding between them. The CO bond dissociation energy of each conformation except for *B4T11* is quite similar to that of $Cr(CO)_6$ calculated by us as well as by Fan and Ziegler[20] with a non-local DF method (147 kJ mol^{-1}) and with the experimental value (162 kJ mol^{-1}) as shown in Table 1.[17]

$$D(\text{Cr–CO}) = E[Cr_2(CO)_5^+] + E[CO] - E[Cr_2(CO)_6^+] \qquad [2]$$

There is room for argument on the point that the relative abundance of $Cr_2(CO)_5^+$ is greater than that of $Cr_2(CO)_6^+$, although the total energy of $Cr_2(CO)_5^+$ is higher (it is more unstable) than that of $Cr_2(CO)_6^+$. Broadly speaking, the formation of the Cr–Cr bond results in an energy gain for the simple association reaction. (Eqn [3]).

Table 6 Total energies for $Cr_2(CO)_6^+$ with respective conformation ($E[Cr_2(CO)_6^+]$, for CO (E[CO]) and for $Cr_2(CO)_5^+$ ($E[Cr_2(CO)_5^+]$) yielded by dissociation reaction of CO from $Cr_2(CO)_6^+$, and dissociation energies for the reaction [D(Cr–C)]

	$E[Cr_2(CO)_6^+]$ (hartree)		E[CO] (hartree)	$E[Cr_2(CO)_5^+]$ (hartree)	D(Cr–C) (kJ mol^{-1})
T33	−2768.5423	C_TO	−113.2651	−2655.2169	−158.3
B2T22	−2768.5283	C_TO	−113.2651	−2655.2011	−163.0
		C_BO	−113.2646	−2655.2040	−156.7
B4T11	−2768.4332	C_TO	−113.2655	−2655.1450	−59.6
		C_BO	−113.2653	−2655.1206	−124.2

$$Cr^+ + Cr(CO)_6 \rightarrow Cr_2(CO)_6^+ \quad [3]$$

For a reaction occurring in the gas phase, the excess energy produced by the reaction that is not taken out must remain as internal energy of the product ion: then the total energy of the reaction system $Cr^+ + Cr(CO)_6$ remains above the dissociation limit. In this case, the product ion must dissociate, releasing the ion Cr^+ again, resulting in no net reaction. However, if some CO is eliminated in reaction [4], some part of the excess energy is consumed in the scission of COs and the net reaction proceeds. When all the excess energy is consumed, the energy gain for the reaction $\Delta E = 0$, i.e. the reaction is thermoneutral. Then the maxima of the distribution of $Cr_2(CO)_n^+$ must occur around the n which satisfies such a condition. Our calculated results describe this mechanism successfully. The bond energy of Cr^+–Cr calculated in our previous study[24] is 146.2 kJ mol^{-1}, almost comparable with each CO bond dissociation energy of *T33* and *B2T22*. Here it is not worthwhile to take *B4T11* into the discussion since the abundance of *B4T11* must be very low, if it is present at all, owing to its instability (it has a higher total energy than the others), as mentioned above. On the assumption that the stabilized energy for structural optimization of $Cr_2(CO)_5^+$ is so small, our results indicate that the excess energy produced by formation of the Cr^+–Cr bond is consumed to eliminate one CO from $Cr_2(CO)_6^+$ to form $Cr_2(CO)_5^+$. Qualitatively, these results are very consistent with those obtained by mass-spectroscopic studies.

$$Cr^+ + Cr(CO)_6 \rightarrow Cr_2(CO)_n^+ + (6-n)CO \quad [4]$$

4 CONCLUSION

Optimized structures and energies for $Cr_2(CO)_6^+$ yielded by the laser ablation–molecular beam (LAMB) method are obtained by density functional calculation with non-local correction using the exchange functional of Becke and correlation functional of Perdew. Calculation was carried out for three conformations with D_{3d} (*T33*), D_{2h} (*B2T22*) and D_{4h} (*B4T11*) symmetries. The difference of conformation exerts a significant influence on the internuclear distance between the chromium and carbon of the terminal CO, but hardly on the Cr–Cr bond length. As for *B2T22* and *B4T11*, longer internuclear distances for bridging carbonyl groups compared with terminal ones indicate an effective π*-back donation from chromium to CO in the bridged form. Furthermore, comparison of the excess energy produced in formation of the Cr^+–Cr bond with the CO bond dissociation energy of $Cr_2(CO)_6^+$ allows us to explain a peculiar feature in the relative abundance of $Cr_2(CO)_n^+$ (n = 0–6) observed in our experimental study.

This calculation constitutes an initial attempt to determine the structures and energies for binuclear metal carbonyl ions which are coordinatively unsaturated. Its verification for reliability should be entrusted to comparison with other calculations by different methods as well as with experiments which will be made in the near future.

DF calculations on mixed-metal carbonyl ions with unsaturated carbonyl groups $MCr(CO)_n^+$ (M = Ti, V, Mn, Fe; n = 0–6) yielded by the LAMB method is under way. Some of our optimized structures and energies for these complex ions will be detailed in our next report.

Acknowledgment We are grateful to Y. Yubuki and M. Sasaki for assistance. This work is partly supported by a Grant-in-Aid (Specially Promoted Research 07102009) from the Ministry of Education, Science and Culture of Japan.

REFERENCES

1. H. Sato, *Res. Chem. Intermed.* **19,** 67 (1993).
2. T. Oka, K. Kasatani, H. Shinohara and H. Sato, *Chem. Lett.* 917 (1991).
3. R. Fournier, *J. Chem. Phys.* **99,** 1801 (1993).
4. E. Folgu and T. Ziegler, *J. Am. Chem. Soc.* **115,** 5169 (1993).
5. J. Li, G. Schreckenbach and T. Ziegler, *J. Phys. Chem.* **98,** 4838 (1994).
6. A. Berces and T. Ziegler, *J. Phys. Chem.* **99,** 11417 (1995).
7. R. Fournier, *J. Chem. Phys.* **98,** 8041 (1993).
8. P. Hohenberg and W. Kohn, *Phys. Rev. B* **136,** 864 (1964).
9. W. Kohn and L. J. Sham, *Phys. Rev. A* **140,** 1133 (1965).
10. A. St-Amant and D. R. Salahub, *Chem. Phys. Lett.* **169,** 387 (1990).
11. D. R. Salahub, R. Fournier, P. Mlynarski, I. Papai, A. St-Amant and J. Ushio, *Density Functional Methods in Chemistry*, Labanowski, J. K. and Andzelm, J. W. (eds), Springer-Verlag, New York, 1991.
12. H. Kobayashi, A. St-Amant, D. R. Salahub and T. Ito, *Proc. 10th Int. Congr. Catal.* 2527 (1993).
13. H. Kobayashi, D. R. Salahub and T. Ito, *J. Phys. Chem.* **98,** 5487 (1994).
14. A. D. Becke, *Phys. Rev. A* **38,** 3098 (1988).
15. J. P. Perdew, *Phys. Rev. B* **33,** 8822 (1992).
16. N. Godbout, D. R. Salahub, J. Andzelm and E. Wimmer, *Can. J. Chem.* **70,** 560 (1992).

17. A. Jost, B. Rees and W. B. Yelon, *Acta Crystallogr. Sect. B* **31,** 2649 (1975).
18. P. Jena, B. K. Rao and S. N. Khanna (eds), *Physcs and Chemistry of Small Clusters*, Plenum, New York, 1987.
19. C. Sosa, J. Andzelm, B. C. Elkin, E. Wimmer, K. D. Dobbs and D. A. Dixon, *J. Phys. Chem.* **96,** 6630 (1992).
20. L. Fan and T. Ziegler, *J. Phys. Chem.* **96,** 6937 (1992).
21. A. Rosa, A. W. Ehlers, E. J. Baerends, J. G. Snijders and G. Te Velde, *J. Phys. Chem.* **100,** 5690 (1996).
22. Yu. M. Efremov, A. N. Samoilova, V. B. Kozhukhovsky and L. V. Gurvich, *J. Mol. Spectrosc.* **73,** 430 (1978).
23. C. W. Bauschlicher Jr, *J. Chem. Phys.* **84,** 872 (1986).
24. H. Sato, K. Kasatani, T. Oka, A. Matsuzaki, S. Nishio, K. Furukawa, T. Wada, T. Yada, S. Hayashi, H. Kobayashi and T. Yamabe, *Appl. Organometal. Chem.* **11,** 913 (1997).

